A molecular portrait of *de novo* genes

Vakirlis N[1,§], Hebert AS[2,6], Opulente DA[3], Achaz G[4,5], Hittinger CT[3,6], Fischer G[1*], Coon JJ[2,6,7,8,9 *] and Lafontaine I[1,¥*]

[*]:corresponding authors: Gilles Fischer gilles.fischer@upmc.fr, Joshua J Coon jcoon@chem.wisc.edu and Ingrid Lafontaine ingrid.lafontaine@upmc.fr

Keywords: new genes, yeasts, evolution, gene birth, *de novo* gene emergence, protein expression

Affiliations:

[1]: Sorbonne Universités, UPMC Univ. Paris 06, CNRS, Institut de Biologie Paris-Seine, Laboratory of Computational and Quantitative Biology, F-75005, Paris, France
[2]: Genome Center of Wisconsin, University of Wisconsin-Madison, USA
[3]: Laboratory of Genetics, Genome Center of Wisconsin, J. F. Crow Institute for the Study of Evolution, Wisconsin Energy Institute, University of Wisconsin-Madison, USA
[4]: Atelier de BioInformatique - ISyEB UMR7205 Muséum National d'Histoire Naturelle, Paris, France
[5]: SMILE group, CIRB UMR7241, Collège de France, Paris, France
[6]: DOE Great Lakes Bioenergy Research Center, University of Wisconsin-Madison, USA
[7]: Department of Biomolecular Chemistry, University of Wisconsin-Madison, USA
[8]: Department of Chemistry, University of Wisconsin-Madison, USA
[9]: Morgridge Institute for Research, Madison, USA
[§]: Present adress: Smurfit Institute of Genetics, Department of Genetics, Trinity College Dublin, University of Dublin, Ireland
[¥]: Present adress: Institut de Biologie Physico-Chimique, UMR7141 CNRS-UPMC Univ. Paris 06, Paris 75005, France and [4]

What is the source of new genes? What fuels genetic innovation, the substrate of long-term adaptation? The mechanism of gene acquisition by *de novo* emergence from previously non-coding sequences, has long been considered as highly improbable[1]. New genes were assumed to mostly appear by gene duplication and divergence[2] or by horizontal gene transfer[3]. In the last decade, only a handful of *de novo* genes have been functionally characterized[4–8], exemplifying their contribution to evolutionary innovations. However, the quantitative importance of *de novo* emergence and a proper description of the dynamics of emergence are still lacking, mainly due to the difficulty of distinguishing *de novo* candidates from highly diverged homologs, from wrongly annotated protein coding genes, and from genes acquired horizontally from remote species. Here we address these issues by using a multi-level systematic approach that carefully selects *de novo* candidates among a set of genes taxonomically restricted to yeast genomes. We predict 703 *de novo* genes in 15 yeast genomes whose phylogeny spans at least 100 million years of evolution[9]. We have validated 82 candidates, by providing new translation evidence for 25 of them through mass spectrometry experiments, in addition to those whose translation has been independently reported previously. Our results establish that *de novo* gene emergence is a widespread phenomenon in the yeast subphylum, only a few being ultimately maintained by selection. As we found that *de novo* genes preferentially arise in GC-rich intergenic regions transcribed from divergent promoters, such as recombination hotspots, we propose a mechanistic model for the early stages of *de novo* gene emergence and evolution in eukaryotes.

Main

Identifying *de novo* genes among Taxonomically Restricted Genes (TRGs) is hampered by the presence of remote homologs, fast evolving sequences, and open reading frames (ORFs)

erroneously annotated as protein coding genes[10]. Here, *de novo* genes were sought for in two yeast genera with high-quality genomes: the *Lachancea*[11], containing both closely related and distant species and the well-characterized much more closely related *Saccharomyces* species[12] (Extended Table 1). Our approach aims at striking a balance between previously published, broader proto-genes surveys[13] and stricter, but more limited approaches such as the ones applied in humans[14]. We first identified 1837 genes with no detectable known homologs outside of the two genera, using the public databases and then inferred the age of each TRG by an improved genomic phylostratigraphy approach[15] (see Methods). We then eliminated 55 fast-diverging homologous TRGs using scores from simulations of protein family evolution. The remaining set was then filtered using a statistical Coding Score (CS) based on codon usage and sequence-based properties (Figure 1a and Extended Figure 1). Finally, we retained 703 *de novo* gene candidates (i.e., TRGs likely to be coding for a protein) derived from an estimated total of 366 events of *de novo* gene creation that took place during the evolution of the two genera. We named the *de novo* candidates "recent" when they were restricted to one species and "ancient" for the others. Taken together, they account for 0.45% of the gene repertoires in *Lachancea* and 0.9% in *Saccharomyces* (Figure 1b, Extended Table 2 and Extended Table 3). Surprisingly, the gene birth rate is constant within each genus, but the average number of events per lineage from root to tip is 31.7 in *Lachancea* and 83.8 in *Saccharomyces* (p=0.0058, Wilcoxon test) (Figure 1c).

We provide experimental evidence of translation for 25 *de novo* genes in *Lachancea* (3 being recent and 22 being ancient) by performing tandem mass spectrometry (MS/MS) analysis at the whole proteome level in rich growth medium conditions (Extended Table 2). Prior global proteomic experiments in *S. cerevisiae* validated 58 out of the 103 *de novo* gene candidates (Extended Table 4).

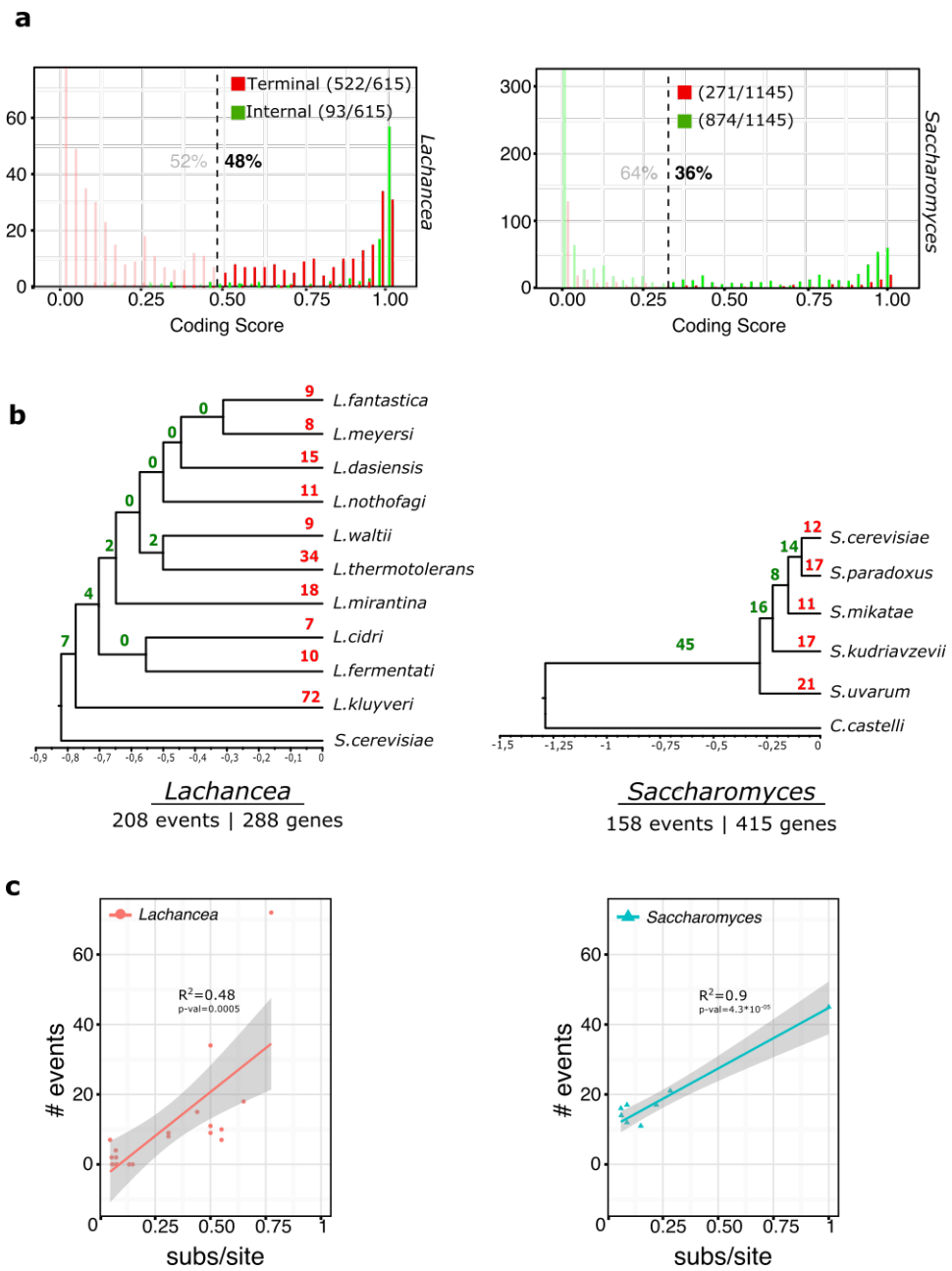

Figure 1. Results of *de novo* gene identification in 2 model yeast genera.
a, Distributions of Coding Scores (CS) of TRGs in the 2 genera. Dashed lines represent thresholds (0.47 in *Lachancea,* 0.3 in *Saccharomyces*) that limit false positives to 5% based on our validation procedure (see Methods and Extended Figure 1). **b,** *De novo* gene origination events along the phylogenies of the 2 genera. Branch lengths correspond to molecular clock estimations of relative species divergence (relative number of substitutions per site) within each genus. Thus, the bottom scale bar expresses species relative number of substitutions per site to the origin of the genus. Recent and ancient events are shown in red and green, respectively. **c,** Numbers of *de novo* creation events as a function of the relative time estimates (per branch) as shown in b.

Altogether experimental evidence of translation validates 83 (12%) of our candidates, which we will refer to as validated *de novo* genes hereafter. Crucially, all validated *de novo* genes have good CS (median at 0.95), suggesting that the latter is a good indicator of protein expression. In total, validated *de novo* genes represent 0.1% of the proteome in yeasts, a significantly higher proportion than what was estimated in other eukaryotes, with 0.01% in *Drosophila*[16], 0.03% in primates[14], and 0.06% in *Plasmodium vivax*[17]. Among the validated *de novo* genes in *S. cerevisiae,* four have a known function: *REC104* and *CSM4* are involved in meiotic recombination, *PEX34* is involved in the peroxisome organization, and *HUG1* participates to the response to DNA replication stress. Although with no characterized function, most of the other validated *de novo* genes are annotated as acting at the periphery of the cell or involved in stress responses (Extended Table 4), suggesting they are involved in sensing of the environment.

The *de novo* candidates share a number of structural properties that differentiate them from the genes conserved outside the two genera. (i) They are significantly shorter than conserved genes (Extended Table 2). (ii) They are more often in opposing orientation with respect to their 5' gene neighbour (Figure 2a). The emergence of a *de novo* gene upstream of an existing gene in the opposite orientation can favour its transcription due to promoter bidirectionality, which is widespread in the baker's yeast[18], as well as in mammals[19] and plants[20]. Furthermore, it provides a nucleosome-free region[21,22] that promotes transcriptional activity. (iii) When recent, *de novo* genes harbor a higher GC content (Figure 2b and Extended Figure 5b and c), even more so when located in opposing orientation with respect to their 5' gene neighbour (Figure 2a right). (iv) When recent, the dN/dS ratio (non-synonymous to synonymous substitution rates) of *de novo* genes is close to 1 and when ancient, the dN/dS gradually decreases down to the level of the one of conserved genes

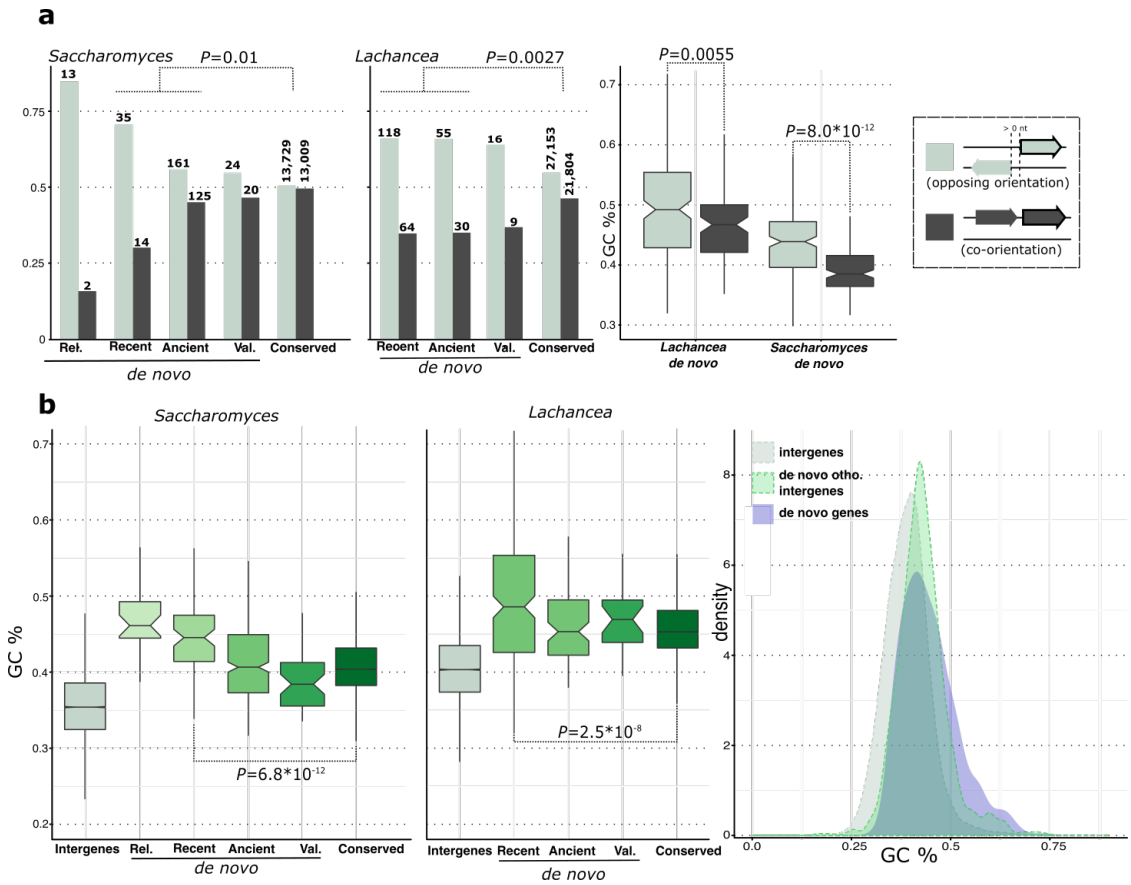

Figure 2. *De novo* genes are enriched at divergent promoters in GC-rich regions
a, Left and middle: Distributions of the transcriptional orientations of various gene classes relative to their 5' neighbours (see text). Only genes with a non-null 5' intergenic spacer (> 0 nt) are considered. Inter.: intergenic regions, Inter. ortho: intergenic regions orthologous to *de novo* genes. Rel: reliable, Val.: validated. Right: GC% distributions of *de novo* genes in opposing and co-orientation configurations in the 2 genera. **b**, Distributions of Guanine-Cytosine percentage (GC%) in various sequence classes. Notches represent the limits of statistical significance.

(Figure 2c). This indicates that the strength of purifying selection increases with gene age at least in *Saccharomyces* (data are insufficient in *Lachancea*). (v) Finally, but *in Lachancea* only, when ancient, *de novo* genes are significantly enriched in disordered segments, relative to conserved genes (Figure 3a and [13]), although they have the same GC content (Figure 2b).

The most convincing evidence of *de novo* gene birth stems from the unambiguous identification of the orthologous non-coding regions from which 30 "reliable" *de novo* genes originated. Using ancestral reconstruction[7], we inferred that each orthologous non-coding region contains one or more ancestral ORF-disrupting nucleotide(s) that once mutated, gave birth to the ORF of the *de novo* gene (Figure 3b and Extended Figure 4). No such mutational scenario could be retrieved in the *Lachancea*, because their genomes are overall very diverged and the orthologous intergenic regions share no longer significant similarity.

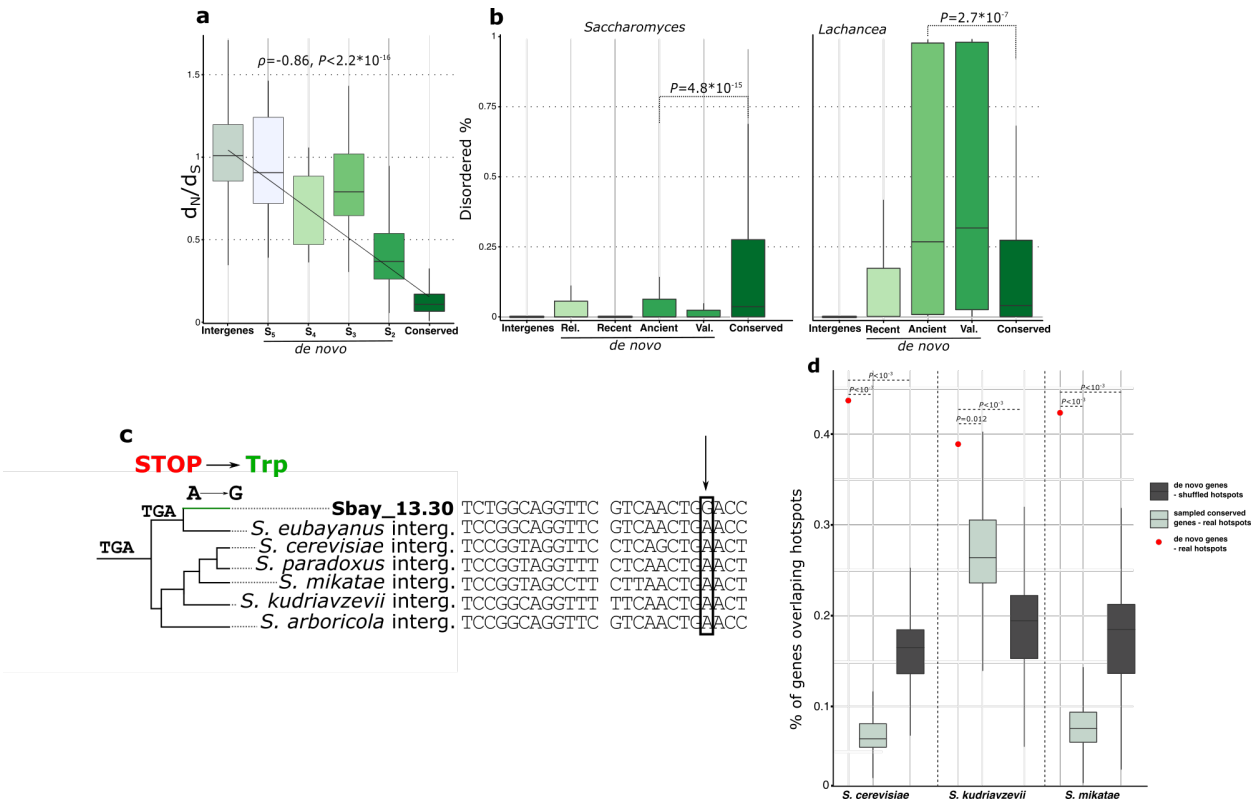

Figure 3. Sequence properties of *de novo* genes
a, Distribution of pairwise dN/dS value for various sequence classes in *Saccharomyces*. S2 to S5 refer to the branches of emergence of *de novo* genes (see Extended Figure 3). **b,** Distributions of percentages of residues in disordered regions for various sequence classes in the 2 genera. Rel.: reliable *de novo* genes for which the ancestral sequence is inferred as non-coding. Val.: validated *de novo* genes with experimental translation evidence. **c**, Part of the alignment of the reliable *de novo* gene *Sbay_13.30* in *S. uvarum* and its orthologous intergenic sequences in 6 *Saccharomyces* genomes. One of the 4 total enabling mutations is indicated with an arrow. Inferred ancestral codons in the position of interest are shown on the ancestral branch of the tree. The entire alignment can be seen in Extended Figure 4. **d,** Proportion of *de novo* genes overlapping recombination hotspots as identified in[23] (outliers are not shown). The 2 null models consist in i) randomly shuffling the hotspots on each chromosome and ii) sampling a set of conserved genes with the same GC composition and chromosome distribution as *de novo* genes. Both models were repeated 1000 times.

Altogether, this suggests that *de novo* emergence tends to occur at the vicinity of divergent promoters in GC-rich non-coding regions, where the probability of finding a fortuitous ORF is the largest (Extended Figure 5a). In multiple eukaryotic taxa, including yeasts and humans,

recombination hotspots (RHS) tend to be GC-rich, because they are subject to biased gene conversion towards GC nucleotides[24–26,23]. In yeasts, RHS also preferentially locate at divergent promoter-containing intergenic regions[26]. They should then be favourable locations for the emergence of *de novo* genes in yeasts. Indeed, in *S. cerevisiae*, *S. mikatae*, and *S. kudriavzevii*, for which recombination maps are exploitable for this study, we found a significant enrichment of *de novo* genes overlapping with RHS[23], including 3 reliable *de novo* genes in *S. kudriavzevii* and 3 in *S. mikatae (*Fig 3c).

Our results strongly argue against the hypothesis that our candidate *de novo* genes where acquired by horizontal transfer from unknown genomes. Firstly, we found the non-coding ancestral sequence of 30 reliable *de novo* genes in *Saccharomyces.* Secondly, documented horizontally transferred genes[27,28,11] are longer than *de novo* genes (Extended Table 5). Lastly, they are not located in opposing orientation with respect to their 5' gene neighbor. Our results also exclude the possibility that our candidates are highly diverged homologs or neo-functionalized duplicates (see Methods).

The role of *de novo* emergence as a potent gene birth mechanism has been much debated during the past decade. In this study, we identified an unprecedented number of *de novo* genes (703 candidates, 76 validated and 30 reliable) across 15 yeasts genomes for which *de novo* emergence is extremely likely. Although, *de novo* emergence occurs at a slow pace, but it is widespread enough that *de novo* genes are present in all genomes studied so far. Importantly, we have in all probability underestimated the number of validated candidates because additional ORFs could actually be expressed in yet untested conditions. Crucially, our observations support a plausible

mechanistic model for the early stages of *de novo* evolution: *de novo* emergence of ORFs occurs within GC-rich regions and can be transcribed from the divergent promoter of the 5' neighbour gene (Figure 4). Most of the newborn genes are lost by genetic drift but few recent ones are recruited for a biological function. Then, as they become more ancient, they enter a regime of purifying selection that, step by step, turns them into canonical genes.

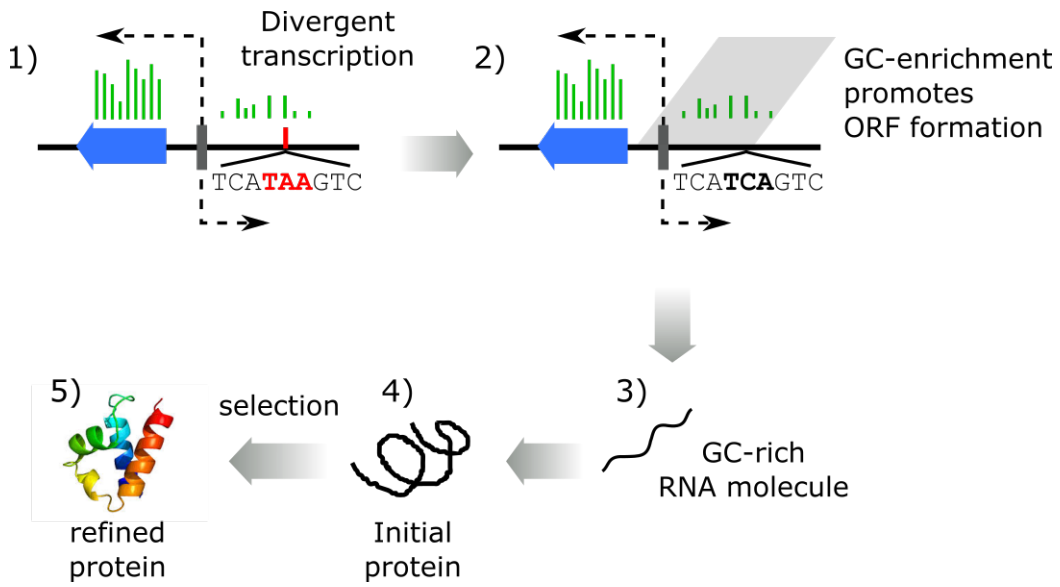

Figure 4. Model of *de novo* genes evolution
Blue arrow: conserved gene. Grey bar: bidirectional promoter. Red bar: stop codon. Green bars: transcription.

References for main section

1. Kaessmann, H. Origins, evolution, and phenotypic impact of new genes. *Genome Research* **20,** 1313–1326 (2010).
2. Ohno, S. *Evolution by Gene and Genome Duplication*. (1970).
3. Lerat, E., Daubin, V., Ochman, H. & Moran, N. A. Evolutionary Origins of Genomic Repertoires in Bacteria. *PLoS Biol* **3,** e130 (2005).

4. Levine, M. T., Jones, C. D., Kern, A. D., Lindfors, H. A. & Begun, D. J. Novel genes derived from noncoding DNA in Drosophila melanogaster are frequently X-linked and exhibit testis-biased expression. *PNAS* **103,** 9935–9939 (2006).
5. Zhou, Q. *et al.* On the origin of new genes in Drosophila. *Genome Res.* **18,** 1446–1455 (2008).
6. Cai, J., Zhao, R., Jiang, H. & Wang, W. De Novo Origination of a New Protein-Coding Gene in Saccharomyces cerevisiae. *Genetics* **179,** 487–496 (2008).
7. Knowles, D. G. & McLysaght, A. Recent de novo origin of human protein-coding genes. *Genome Res.* (2009). doi:10.1101/gr.095026.109
8. Li, D. *et al.* A de novo originated gene depresses budding yeast mating pathway and is repressed by the protein encoded by its antisense strand. *Cell Res.* **20,** 408–420 (2010).
9. Berbee, M. L. & Taylor, J. W. Dating divergences in the fungal tree of life: Review and new analyses. *Mycologia* **98,** 838–849 (2006).
10. Khalturin, K., Hemmrich, G., Fraune, S., Augustin, R. & Bosch, T. C. G. More than just orphans: are taxonomically-restricted genes important in evolution? *Trends in Genetics* **25,** 404–413 (2009).
11. Vakirlis, N. *et al.* Reconstruction of ancestral chromosome architecture and gene repertoire reveals principles of genome evolution in a model yeast genus. *Genome Res.* **26,** 918–932 (2016).
12. Scannell, D. R. *et al.* The Awesome Power of Yeast Evolutionary Genetics: New Genome Sequences and Strain Resources for the Saccharomyces sensu stricto Genus. *G3* **1,** 11–25 (2011).
13. Carvunis, A.-R. *et al.* Proto-genes and de novo gene birth. *Nature* **487,** 370–374 (2012).

14. Guerzoni, D. & McLysaght, A. De Novo Origins of Human Genes. *PLoS Genet* **7,** e1002381 (2011).

15. Domazet-Lošo, T., Brajković, J. & Tautz, D. A phylostratigraphy approach to uncover the genomic history of major adaptations in metazoan lineages. *Trends in Genetics* **23,** 533–539 (2007).

16. Chen, S., Zhang, Y. E. & Long, M. New Genes in Drosophila Quickly Become Essential. *Science* **330,** 1682–1685 (2010).

17. Yang, Z. & Huang, J. De novo origin of new genes with introns in Plasmodium vivax. *FEBS Letters* **585,** 641–644 (2011).

18. Neil, H. *et al.* Widespread bidirectional promoters are the major source of cryptic transcripts in yeast. *Nature* **457,** 1038–1042 (2009).

19. Trinklein, N. D. *et al.* An Abundance of Bidirectional Promoters in the Human Genome. *Genome Res.* **14,** 62–66 (2004).

20. Krom, N. & Ramakrishna, W. Comparative Analysis of Divergent and Convergent Gene Pairs and Their Expression Patterns in Rice, Arabidopsis, and Populus. *PLANT PHYSIOLOGY* **147,** 1763–1773 (2008).

21. Pan, J. *et al.* A hierarchical combination of factors shapes the genome-wide topography of yeast meiotic recombination initiation. *Cell* **144,** 719–731 (2011).

22. Berchowitz, L. E., Hanlon, S. E., Lieb, J. D. & Copenhaver, G. P. A positive but complex association between meiotic double-strand break hotspots and open chromatin in Saccharomyces cerevisiae. *Genome Res* **19,** 2245–2257 (2009).

23. Lam, I. & Keeney, S. Nonparadoxical evolutionary stability of the recombination initiation landscape in yeast. *Science* **350,** 932–937 (2015).

24. Lamb, B. C. The properties of meiotic gene conversion important in its effects on evolution. *Heredity (Edinb)* **53 (Pt 1),** 113–138 (1984).

25. Jeffreys, A. J. & Neumann, R. Reciprocal crossover asymmetry and meiotic drive in a human recombination hot spot. *Nat Genet* **31,** 267–271 (2002).

26. Mancera, E., Bourgon, R., Brozzi, A., Huber, W. & Steinmetz, L. M. High-resolution mapping of meiotic crossovers and noncrossovers in yeast. *Nature* **454,** 479–485 (2008).

27. Rolland, T., Neuvéglise, C., Sacerdot, C. & Dujon, B. Insertion of horizontally transferred genes within conserved syntenic regions of yeast genomes. *PLoS ONE* **4,** e6515 (2009).

28. Marcet-Houben, M. & Gabaldón, T. Acquisition of prokaryotic genes by fungal genomes. *Trends in Genetics* **26,** 5–8 (2010).

Methods

Data collection

We investigated *de novo* gene emergence in 10 *Lachancea* and 5 *Saccharomyces* genomes (*L. kluyveri*, *L. fermentati*, *L. cidri*, *L. mirantina*, *L. waltii*, *L. thermotolerans*, *L. dasiensis*, *L. nothofagi*, "*L. fantastica*" nomen nudum and *L. meyersii*, *S. cerevisiae*, *S. paradoxus*, *S. mikatae*, *S. kudriavzevii*, and *S. bayanus* var. *uvarum*), see Extended Table 1. For the *Saccharomyces*, the genome of *S. arboricola* was not analysed because it contains *ca.* half of the number of annotated genes as the others. It was only used for the reconstruction of the ancestral sequences of *de novo* genes. The genome of *S. eubayanus* was not analysed either because it was not annotated with the same pipeline. It was used for the reconstruction of the ancestral sequences of *de novo* genes and for the simulation of the protein families' evolution. For outgroup species references, the

genomes *Kluyveromyces marxianus*, *K. lactis,* and *K. dobzhanskii* were used for the *Lachancea* and the genomes of *Candida castellii* and *Nakaseomyces bacilisporu*s were used for the *Saccharomyces*. The sources for genome sequences and associated annotations are summarized in Supplementary Information. Annotated CDS longer than 150 nucleotides were considered.

The high raw coverages of the assembled genomes in the two genera minimized erroneous base calls and makes sequencing errors and subsequent erroneous *de novo* assignment very unlikely (N50 values range from 801 to 905 kb for *Saccharomyces*[1] and form 1275 and 2184 kb in *Lachancea*). The combined 454 libraries and Illumina single-reads for the *Lachancea* further allowed the correction of sequencing errors in homopolymer blocks that generated erroneous frameshifts in genes.

Pipeline for TRG detection

Initially, the protein sequences of all considered species (focal proteome) are compared against each other using BLASTP[2] (version 2.2.28+, with the options *-use_sw_tback -comp_based_stats* and an E-value cut-off of 0.001) then clustered into protein families by TribeMCL[3] (version 12-068, I=6.5) based on sequence similarity, as previously reported for the *Lachancea* genomes[4]. For each family, a multiple alignment of the translated products is generated (see *General procedures* section) and profiles (HMM and PSSM) are built from it. These first steps are also performed for the proteome of the outgroup species.

A similarity search for homologs outside of the focal species is then performed against the NCBI nr database with BLASTP for singletons and with PSI-BLAST version 2.2.28+ for families with the PSSM profile of the corresponding family. Hits are considered significant if they have an e-value lower than 0.001 for both BLASTP and PSI-BLAST. A family (or singleton) is considered

as taxonomically restricted if it has no significant hit in nr. This work was already done previously[4] for *Lachancea*. TRGs whose coordinates overlapped conserved genes on the same strand were removed.

Next, TRG families are searched against each other using HMM profile-profile comparisons with the HHSUITE programs version 2.0.16[5]. HMM profiles were built with *hhmake*, and database searches were performed with *hhsearch*. A hit is considered significant if it has a probability higher than 0.8 and an E-value lower than 1, values previously defined as optimal[6]. Families sharing significant similarity are merged. This new set of TRG families is used to search for similarity in 4 databases: an HMM profile database built from the alignments of the genus' conserved families, the profile database of the outgroup species, the PDB70 profile database (version of 03-10-2016)[7], and the PFAM profile database (version 27.0)[8]. Singleton TRGs were compared by sequence-profile searches using *hmmscan* of the HMMER3 package version 3.1b2 [9] (E-value cut-off 10^{-5}) in all the above databases, except PDB70. The final curated TRG families are those for which no significant match is found in any searched database. Finally, the branch of origin of each TRG family is inferred as the branch leading to the most recent common ancestor of the species in which a member of the family is present. The reference species phylogeny is given in Extended Figure 3.

Simulations of protein family evolution

To simulate protein family evolution along a given species phylogeny, we followed a slightly modified version of the methodology used by Moyers *et al.*[10,11]. The real orthologous gene families were defined as families of syntenic homologues with only one member per species as in Vakirlis *et al.*[4]. We defined 3668 such families across the 10 *Lachancea* and their 3 outgroup

species, as well as 3946 families across the 6 *Saccharomyces* species and their 2 outgroup species. We modified the protocol of Moyers et al. in two ways: we inferred protein evolutionary rates for each individual gene tree (branch lengths representing substitutions per 100 sites), instead of calculating the mean evolutionary rate of a protein by the number of substitutions per site per million years between a couple of yeast species, and we did so using the PAM matrix (instead of the Jones-Taylor-Thornton one used by Moyers et al.), which is the only readily available matrix in the ROSE program version 1.3[12]. We performed simulations under two scenarios. In the first scenario, the amount of divergence within each simulated protein family mirrors the one within real orthologous families (normal case). In the second scenario, the divergence is 30% higher than the one estimated among the real orthologous families (every simulated branch is 30% longer than its real equivalent), and additionally, for each branch, there is a factor that adds a random amount of extra divergence ranging from 0 to 100% of the branch's length (worst case). The phylogenetic distances between real homologous members and between members of simulated families are similar in each scenario (see Extended Figure 6). At the end of each simulation, we inferred the evolutionary relationships using our pipeline for TRG detection described above (Extended Figure 7). Briefly, our results show that even under a worst-case scenario, false positives cannot explain the total percentages of real TRGs. This essentially demonstrates that sequence divergence alone is not responsible for the observed patterns of presence and absence of genes.

Sequence properties

Codon usage and Codon Adaptation Index (CAI) values for protein coding sequences were calculated with the CAIJAVA program version 1.0[13] (which does not require any set of reference sequences) with 15 iterations. CAI for the intergenic sequences was calculated with codonW

version 1.3[14] afterwards, based on codon usage of genes with CAI > 0.7 (a CAIJava calculated), so as to get the values that correspond to the previously estimated codon usage bias of the coding genes and not a bias that may be present within intergeninc regions.

The expected number of amino acids in a transmembrane region were calculated with the TMHMM program[15]. Disordered regions were defined as protein segments not in a globular domain and were predicted with IUPRED version 1.0[16].

Low complexity regions were detected with *segmasker* version 1.0.0 from the BLAST+ suite. Biosynthesis costs were calculated using the Akashi and Gojobori scores[17,18]. GRAnd AVerage of Hydropathy (GRAVY) and aromaticity scores of each protein sequence were calculated with codonW version 1.3. Predictions of helices and sheets in protein sequences were obtained by PSIPRED version 3.5[19] in single sequence mode. TANGO version 2.3[20] was used to predict the mean aggregation propensity per residue for all proteins with the settings provided in the tutorial examples.

Calculation of Coding Score

We built a binomial logistic regression classifier on a Coding class and a Non-coding class. The Coding class sequences are genes conserved inside and outside of the focal genus. The Non-coding sequences corresponding to the +1 reading frame of intergenic regions in which in-frame stop codons were removed. All non-annotated regions were considered in the *Lachancea* genomes, while orthologous intergenic regions are available at www.SaccharomycesSensuStricto.org[1] where considered in the *Saccharomyces* genomes. Each class have equal sizes (6000 sequences each), which are sampled to have approximately the same length distribution. The Coding Score is the model's fitted probability for the Coding class. The

classifier was trained on the following sequence feature data: frequencies of 61 codons, CAI, biosynthesis cost, percentage of residues in i) transmembrane regions ii) disordered regions ii) low complexity regions iv) helices v) beta sheets, hydrophobicity scores, aromaticity scores, mean aggregation propensity per residue and the GC·GC3 term, where GC is the percentage of Guanine-Cytosine bases and $GC3$ is the percentage of Guanine-Cytosine bases at the 3rd codon position.

$$\mathrm{GC{\cdot}GC3} = \frac{|GC - GC3|}{|GC3 - 0.5|}$$

Each feature was standardized by subtracting the mean and dividing by the standard deviation. The binomial logistic regression classifier was constructed with the GLMNET R package version 2.0-2[21], with an optimized alpha value (0.3 and 0.4 for the *Lachancea* and for the *Saccharomyces*, respectively) estimated by testing on a separate validation set of coding and non-coding sequences, and keeping the value that minimized the class prediction error. The function *cv.glmnet* with the optimal alpha value was used on the training set to perform 10-fold cross-validation to select and fit the model that minimizes the class prediction error for a binomial distribution. Validation of the performance of the coding score is given in Extended Figure 6.

Orientation analysis

Relative orientation of the 5' transcribed element was considered, and a gene was tagged either in oppsoing orientation (<– –>) if its 5' neighbor is transcribed on the opposite strand or co-oriented (–> –>) if its 5' neighbor is transcribed on the same strand. Only genes that do not overlap other elements on the opposite strand at their 5' extremity (non-null intergenic spacer)

were considered. Relative 5' orientations were determined for *de novo* genes, conserved genes and tandem duplicated genes. Tandemly duplicated genes are paralogs that are contiguous on the chromosome. *De novo* genes are significantly enriched in opposing orientation (<- ->) (Figure 2e) while tandem duplicated genes are significantly enriched in a co-orientation (638 and 428 in *Saccharomyces* and *Lachancea*, respectively) with only 287 and 152 tandemly duplicated genes in opposing orientation in *Saccharomyces* and *Lachancea*, respectively. This inversed bias states that our *de novo* gene candidates do not actually correspond to tandemly duplicated genes that diverged beyond recognition, thus the duplication-divergence model does not apply to our *de novo* candidates[22].

Similarity searches in intergenic regions

For each chromosome, low complexity regions were first masked with *segmasker* version 1.0.0 and annotated regions were subsequently masked by *maskfeat* from the EMBOSS package version 6.4.0.0 [23]. Similarity searches between all 6 frame translations of the masked chromosome sequences and the TRG protein sequences allowing for all kinds of mutations and frameshifts were performed with the *fasty36*[24] binary from the FASTA suite of tools version 36.3.6 with the following parameters: BP62 scoring matrix, a penalty of 30 for frame-shifts and filtering of low complexity residues. Significant hits (30% identity, 50% target coverage and an E-value lower than 10^{-5}) in at least two genomes within an intergenic region that are syntenic to a *de novo* gene were selected and their corresponding DNA regions were extracted. A multiple alignment was then performed and in-frame stop codons where searched in the phase whose translation is similar to the *de novo* gene product. All gaps that were not a multiple of three were considered as indels. In 16 cases, the enabling mutations from the ancestral non-coding sequence can be precisely traced forward based on the multiple alignment, as in Knowles and Mclysaght[25]

Evolutionary analyses

For each TRG family with members in at least two different species, rates of synonymous substitutions (dS) and rates of non-synonymous substitutions (dN) were estimated from protein guided nucleotide alignments with the *codeml* program from the PAML package version 4.7[26]. Pairwise analyses were done using the Yang and Nielsen model[27]. The relative rates dN/dS values were considered only if the standard error of dN and the standard error of dS were lower than dN/2 and dS/2 respectively and dS was lower than 1.5. Ancestral sequences were calculated with *baseml* from the PAML package version 4.7 using the REV model.

Relative divergence estimates

Timetrees for both *Lachancea* and *Saccharomyces* were generated using the RelTime method[28]. For each genera, we selected 100 families of syntenic homologs present in every genome for which the inferred tree has the same topology as the reference species tree[1,4]. The concatenation of the protein-guided cDNA alignments of the family of syntenic homologs present in each genomes (in the 10 *Lachancea* or in the 5 *Saccharomyces*) were given as input. As outgroup species, we used *S. cerevisiae* for the *Lachancea* and *Candida castellii* for the *Saccharomyces*. 7759 and 74663 sites were used for the *Saccharomyces* and for the *Lachancea*, respectively. Divergence times for all branching points in the topology were calculated using the Maximum Likelihood method based on the Tamura-Nei model[29]. 3rd codon positions were considered. All positions containing gaps and missing data were eliminated. Evolutionary analyses were conducted in MEGA7[30].

We found that, in both genera, branch lengths correlate to the number of *de novo* emergence events (linear regression lines in inset plot) suggesting that *de novo* emergence occurs at a coordinated pace with non-synonymous mutations. Although this correlation is probably true, the limited number of data points means that these results are best viewed qualitatively and with caution. In other words, the slopes of the fitted regression lines are unlikely to represent the true emergence rates.

Recombination hotspots analysis

Recombination maps were retrieved from[31]. The strains used to determine the recombination maps are those also used in this study[1], so the same assembly has been used to map the Spo11 oligos for the recombination map and to detect *de novo* genes. This is not the case for *S. paradoxus*, because the recombination map is constructed for the YPS138 strain, which is quite divergent from the *S. paradoxus* strain CBS432 used to detect *de novo* genes, and for which only a low quality assembly is available. In *S. cerevisiae*, *S. mikatae* and *S. kudriavzevii* more than 38% (44%, 42% and 39% respectively) of *de novo* genes overlap with RHS on at least 10% of their length, with an average overlap of 65% (204 nt), 66% (192 nt) and 42% (178 nt) of the gene length in the three species, respectively. This is more than a 3-fold enrichment compared to 2 null models: 1) *de novo* genes overlapping with a null model of random, shuffled hotspot-equivalent regions and 2) a null model of sampled conserved genes with the same GC content, length and chromosome distribution as *de novo* genes overlapping with the real set of RHS (P-value<0.001 calculated from 1000 simulations for all tests, except for *S. kudriavzevii* in the sampled conserved test, P-value = 0.012). There is no enrichment in *S. paradoxus* but as mentioned above, no conclusion can be made because of the divergence between the strain used for the recombination map and the strain used to detect *de novo* genes.

General procedures

All alignments were done with the MAFFT *linsi* executable (version 7.130b)[34]. All statistical analyses were done in R version 3.1[35] with standard library functions unless otherwise noted. Phylogenetic distances from protein family alignments were calculated using *fprotdist* from the EMBOSS version 6.4.0.0 with the PAM matrix and uniform rate for all sites (-ncategories 1). The PAM matrix was chosen for consistency.

Translation evidence

De novo genes in *S. cerevisiae* for which positive proteomic data are available MS are tagged as "with translation evidence". This designation corresponds to protein products identified i) in MS-based proteome characterization studies, ii) as prey proteins in MS-based affinity capture studies, iii) in two-hybrid experiments, iv) as localized by fluorescent fusion protein constructs, v) as a substrate in phosphorylation assays, vi) identified in ribosome profiling experiments and/or vii) in protein-fragment complementation assays.

Mass spectrometry protocol

Cell culture and sample preparation

Single colonies of each species were inoculated in 3 mL YP + 2% Glucose and grown at 30_C. After 2 days growth, the liquid cultures were inoculated into 12mL of YP + 2% Glucose at 30_C and were grown until they reached an optical density of 1.0. Cultures were centrifuged at 4,000 RPM for 2 minutes and the supernatant was removed. The cells were washed in 1ml of 1M Sorbitol and centrifuged for 2 minutes at 15,000 RPM. The supernatant was removed and the cells were stored at -80 °C.

1

2 ### Lysis and digestion

3 For each strain three biological replicates were analysed. Cells were resuspended in 100 µL 6 M
4 GnHCl, followed by addition of 900 µL MeOH. Samples were centrifuged at 15,000 g for 5 min.
5 Supernatant was discarded and pellets were allowed to dry for ~5 min. Pellets were resuspended
6 in 200 µL 8 M urea, 100 mM Tris pH 8.0, 10 mM TCEP, and 40 mM chloroacetamide, then
7 diluted to 1.5 M urea in 50 mM Tris pH 8[36]. Trypsin was added at 50:1 ratio, and samples were
8 incubated overnight at ambient temperature. Each sample was desalted over a PS-DVB solid
9 phase extraction cartridge and dried down. Peptide mass was assayed with the peptide
10 colorimetric assay (Thermo, Rockford).

11 ### LC-MS/MS

12 For each analysis, 2 µg of peptides were loaded onto a 75 µm i.d. 30 cm long capillary with an
13 imbedded electrospray emitter and packed with 1.7 µm C18 BEH stationary phase. Peptides
14 were eluted with in increasing gradient of acetonitrile over 100 min[37].

15 Eluting peptides were analysed with an Orbitrap Fusion Lumos. Survey scans were performed at
16 R = 60,000 with wide isolation 300-1,350 mz. Data dependent top speed (2 seconds) MS/MS
17 sampling of peptide precursors was enabled with dynamic exclusion set to 15 seconds on
18 precursors with charge states 2 to 6. MS/MS sampling was performed with 1.6 Da quadrupole
19 isolation, fragmentation by HCD with NCE of 30, analysis in the Orbitrap with R = 15,000, with
20 a max inject time of 22 msec, and AGC target set to 2 x 10^5.

21 ### Analysis

22 Raw files were analysed using MaxQuant 1.5.2.8[38]. Spectra were searched using the Andromeda
23 search engine against a target decoy databases provided for each strain independently. Default
24 parameters were used for all searches. Peptides were grouped into subsumable protein groups

and filtered to 1% FDR, based on target decoy approach[38]. For each strain, the sequence coverage and spectral count (MS/MS count) was reported for each protein and each replicate, as well as the spectral count sum of all replicates.

The *de novo* genes that are translated are homogeneously distributed across the 10 *Lachancea* species (P=0.6, X^2 test). The proportion of *de novo* genes detected (25/288, 8.7%) is significantly lower than that of conserved genes of similar length (66%), which by definition appeared before the most ancient *de novo* genes. This depletion could be due to *de novo* genes only being expressed under particular conditions or stresses that were not tested in our experiments. Conversely, MS/MS did not detect TRG eliminated as spurious by our procedure.

Data Availability

Raw data is available on the chorus project (www.chorusproject.org) public experiment "Lachancea de novo" ID# 2884."

References for Methods section

1. Scannell, D. R. *et al.* The Awesome Power of Yeast Evolutionary Genetics: New Genome Sequences and Strain Resources for the Saccharomyces sensu stricto Genus. *G3* **1,** 11–25 (2011).

2. Altschul, S. F., Gish, W., Miller, W., Myers, E. W. & Lipman, D. J. Basic local alignment search tool. *J. Mol. Biol.* **215,** 403–410 (1990).

3. Enright, A. J., Van Dongen, S. & Ouzounis, C. A. An efficient algorithm for large-scale detection of protein families. *Nucleic Acids Res.* **30,** 1575–1584 (2002).

4. Vakirlis, N. *et al.* Reconstruction of ancestral chromosome architecture and gene repertoire reveals principles of genome evolution in a model yeast genus. *Genome Res.* (2016). doi:10.1101/gr.204420.116

5. Söding, J. Protein homology detection by HMM-HMM comparison. *Bioinformatics* **21,** 951–960 (2005).

6. Lobb, B., Kurtz, D. A., Moreno-Hagelsieb, G. & Doxey, A. C. Remote homology and the functions of metagenomic dark matter. *Front Genet* **6,** (2015).

7. Söding, J., Biegert, A. & Lupas, A. N. The HHpred interactive server for protein homology detection and structure prediction. *Nucleic Acids Res.* **33,** W244-248 (2005).

8. Finn, R. D. *et al.* Pfam: the protein families database. *Nucl. Acids Res.* **42,** D222–D230 (2014).

9. Mistry, J., Finn, R. D., Eddy, S. R., Bateman, A. & Punta, M. Challenges in homology search: HMMER3 and convergent evolution of coiled-coil regions. *Nucl. Acids Res.* **41,** e121–e121 (2013).

10. Moyers, B. A. & Zhang, J. Phylostratigraphic bias creates spurious patterns of genome evolution. *Mol Biol Evol* msu286 (2014). doi:10.1093/molbev/msu286

11. Moyers, B. A. & Zhang, J. Evaluating Phylostratigraphic Evidence for Widespread De Novo Gene Birth in Genome Evolution. *Mol Biol Evol* **33,** 1245–1256 (2016).

12. Stoye, J., Evers, D. & Meyer, F. Rose: generating sequence families. *Bioinformatics* **14,** 157–163 (1998).

13. Carbone, A., Zinovyev, A. & Képès, F. Codon adaptation index as a measure of dominating codon bias. *Bioinformatics* **19,** 2005–2015 (2003).

14. Correspondence Analysis of Codon Usage. Available at: http://codonw.sourceforge.net/. (Accessed: 7th June 2016)

15. Krogh, A., Larsson, B., von Heijne, G. & Sonnhammer, E. L. Predicting transmembrane protein topology with a hidden Markov model: application to complete genomes. *J. Mol. Biol.* **305,** 567–580 (2001).

16. Dosztányi, Z., Csizmok, V., Tompa, P. & Simon, I. IUPred: web server for the prediction of intrinsically unstructured regions of proteins based on estimated energy content. *Bioinformatics* **21,** 3433–3434 (2005).

17. Akashi, H. & Gojobori, T. Metabolic efficiency and amino acid composition in the proteomes of Escherichia coli and Bacillus subtilis. *Proc. Natl. Acad. Sci. U.S.A.* **99,** 3695–3700 (2002).

18. Barton, M. D., Delneri, D., Oliver, S. G., Rattray, M. & Bergman, C. M. Evolutionary Systems Biology of Amino Acid Biosynthetic Cost in Yeast. *PLOS ONE* **5,** e11935 (2010).

19. McGuffin, L. J., Bryson, K. & Jones, D. T. The PSIPRED protein structure prediction server. *Bioinformatics* **16,** 404–405 (2000).

20. Fernandez-Escamilla, A.-M., Rousseau, F., Schymkowitz, J. & Serrano, L. Prediction of sequence-dependent and mutational effects on the aggregation of peptides and proteins. *Nat. Biotechnol.* **22,** 1302–1306 (2004).

21. Regularization Paths for Generalized Linear Models via Coordinate Descent | Friedman | Journal of Statistical Software. Available at: https://www.jstatsoft.org/article/view/v033i01. (Accessed: 7th June 2016)

22. Ohno, S. *Evolution by Gene and Genome Duplication*. (1970).

23. Rice, P., Longden, I. & Bleasby, A. EMBOSS: the European Molecular Biology Open Software Suite. *Trends Genet* **16,** 276–7 (2000).

24. Pearson, W. R., Wood, T., Zhang, Z. & Miller, W. Comparison of DNA sequences with protein sequences. *Genomics* **46,** 24–36 (1997).

25. Knowles, D. G. & McLysaght, A. Recent de novo origin of human protein-coding genes. *Genome Res.* (2009). doi:10.1101/gr.095026.109

26. Yang, Z. PAML 4: Phylogenetic Analysis by Maximum Likelihood. *Mol Biol Evol* **24,** 1586–1591 (2007).

27. Yang, Z. & Nielsen, R. Estimating Synonymous and Nonsynonymous Substitution Rates Under Realistic Evolutionary Models. *Mol Biol Evol* **17,** 32–43 (2000).

28. Tamura, K. *et al.* Estimating divergence times in large molecular phylogenies. *PNAS* **109,** 19333–19338 (2012).

29. Tamura, K. & Nei, M. Estimation of the number of nucleotide substitutions in the control region of mitochondrial DNA in humans and chimpanzees. *Mol. Biol. Evol.* **10,** 512–526 (1993).

30. Kumar, S., Stecher, G. & Tamura, K. MEGA7: Molecular Evolutionary Genetics Analysis Version 7.0 for Bigger Datasets. *Mol Biol Evol* **33,** 1870–1874 (2016).

31. Lam, I. & Keeney, S. Non-paradoxical evolutionary stability of the recombination initiation landscape in yeast. *Science* **350,** 932–937 (2015).

32. Lorenz, R. *et al.* ViennaRNA Package 2.0. *Algorithms for Molecular Biology* **6,** 26 (2011).

33. Jiang, M., Anderson, J., Gillespie, J. & Mayne, M. uShuffle: A useful tool for shuffling biological sequences while preserving the k-let counts. *BMC Bioinformatics* **9,** 192 (2008).

34. Katoh, K. & Standley, D. M. MAFFT Multiple Sequence Alignment Software Version 7: Improvements in Performance and Usability. *Mol Biol Evol* **30,** 772–780 (2013).

35. R Core Team. *R: A Language and Environment for Statistical Computing*. (R Foundation for Statistical Computing, 2014).

36. Carvunis, A.-R. *et al.* Proto-genes and de novo gene birth. *Nature* **487,** 370–374 (2012).

37. Hebert, A. S. *et al.* The one hour yeast proteome. *Mol. Cell Proteomics* **13,** 339–347 (2014).

38. Cox, J. & Mann, M. MaxQuant enables high peptide identification rates, individualized p.p.b.-range mass accuracies and proteome-wide protein quantification. *Nat. Biotechnol.* **26,** 1367–1372 (2008).

Acknowledgments

We thank the Agence Nationale de la Recherche (Grant GB-3G, ANR-10-BLAN-1606), the CNRS (Grant PEPS ExoMod Neo-Gene), the USDA National Institute of Food and Agriculture (Hatch Project 1003258), the National Science Foundation (Grant No. DEB-1442148), the DOE

Great Lakes Bioenergy Research Center (DOE BER Office of Science DE-FC02-07ER64494) and the National Institutes of Health (Grant P41GM108538) for financial support. CTH is a Pew Scholar in the Biomedical Sciences, supported by the Pew Charitable Trusts. We thank M. Bailly-Bechet, A. Lambert, S. Lemaire, O. Namy, and C. Neuvéglise for help in the analysis of the results and for discussing unpublished data. We thank F. Barras, Y. Choquet, B. Dujon, R. Lavery, E. Rocha, and F.A. Wollman for fruitful discussions and critical reading of the manuscript.

Contributions

NV and IL performed the bioinformatics experiments. ASH performed spectrometry experiments and analysed the spectrometry results. DAO prepared the biological samples. GA performed the probality estimates. ASH and DAO corrected the manuscript. GA, CTH, JJC and GF contributed to the conception of the experiments, to the interpretation of the results and to the writing of the manuscript. NV and IL conceived the experiments, interpreted the results and wrote the manuscript.